THE ASTROPHYSICAL JOURNAL, 469:715–718, 1996 October 1

APPROXIMATE ANALYTICAL EXPRESSIONS OF THE WIND-DRIVEN BOW SHOCK

YANG CHEN
Department of Astronomy, Nanjing University, Nanjing 210093, China; postcstd@nju.edu.cn
RINO BANDIERA
Osservatorio Astrofisico di Arcetri, Largo Enrico Fermi 5, I-50125 Firenze, Italy; bandiera@arcetri.astro.it
AND
ZHEN-RU WANG
Department of Astronomy, Nanjing University, Nanjing 210093, China, and Center of Astronomy and Astrophysics, CCAST World Laboratory, P.O. Box 8730, Beijing 100080, China; zrwang@nju.edu.cn
Received 1996 February 15; accepted 1996 April 16

ABSTRACT

Previous analytical works on the wind-driven thin-shell bow shock neglected the centrifugal force exerted on the shell material. We reanalyze the dynamic equations including the centrifugal force, and we present approximate formulae in a Cartesian coordinate system for the general quantities describing the thin-shell bow shock. The shocked interstellar medium and the shocked stellar wind are treated as mixed and separated, respectively. These formulae are more accurate than previous analytical results.

Subject headings: ISM: kinematics and dynamics — methods: analytical — shock waves — stars: early-type — stars: mass loss

1. INTRODUCTION

More and more nebulae of cometary morphology have been discovered around mass-losing stars such as early-type O stars, supergiants, Wolf-Rayet stars, cataclysmic binaries, pulsars, etc., by radio, infrared, optical, and even X-ray observations. They were proposed to be bow shock structures which are usually the results of the collision of a stellar wind with a plane-parallel moving interstellar medium (ISM). A bow shock is formed ahead of the star, with a nebula of trailing configuration, when the star moves with respect to the ISM at a supersonic velocity v_*. A variety of algorithms have been developed to describe the dynamics of the bow shock. They can essentially be divided into two sorts, namely, numerical and analytical treatments.

Baranov, Krasnobaev, & Kulikovskii (1971), Baranov, Lebedev, & Ruderman (1979), and Aldcroft, Romani, & Cordes (1992) calculated numerically in a polar coordinate system, while Huang & Weigert (1982), Bandiera (1993), and Chen, Wang, & Qu (1995) calculated in a Cartesian coordinate system. Matsuda et al. (1989) and Mac Low et al. (1991) simulated numerically the bow shock in different ways.

Under the thin-shell approximation (Baranov et al. 1971; Huang & Weigert 1982), analytical studies were carried out. Figure 1 shows the inertial reference frame in which the bow shock solution is stationary, with position angle θ defined there. The origin of the coordinates is set at the position of the star, and the parabolic arc (*solid line*) stands for the contact discontinuity. G_1 and G_2 denote the regions of shocked ISM and shocked wind, respectively. Dyson (1975) derived an approximate solution for the morphology of the contact discontinuity in a tricky way:

$$\frac{r}{r_0} = \frac{\theta}{\sin\theta}, \tag{1}$$

where r_0 is referred to as the standoff distance of the stagnation point. This solution was also obtained by Houpis & Mendis (1980) in their study of cometary ionospheres. It was expanded into Taylor series for $y \ll r_0$ by Mac Low et al. (1991):

$$1 + \frac{x}{r_0} = \frac{1}{3}\left(\frac{y}{r_0}\right)^2. \tag{2}$$

This expansion applies only near the apex (see Fig. 2), though it is better than the approximation $1 + x/r_0 = (y/r_0)^2$ of Van Buren & McCray (1988). Equation (1) and its inferences for physical quantities have been adopted extensively (e.g., Van Buren et al. 1990; Borkowski, Blondin, & Sarazin 1992; Raga & Cabrit 1993; Wang, Dyson, & Kahn 1993; Raga, Cabrit, & Cantó 1995). In order to derive the analytical solution, however, Dyson (1975) and Houpis & Mendis (1980) neglected the term describing the centrifugal force due to the curvature motion of the mass flow in the shell, making the morphology of the bow shock shell more curved than the exact solution (see Fig. 2). Moreover, they derived the solutions only for small θ ($\lesssim 70°$) and considered only the case in which $v_w \ll v_*$ (therefore actually neglecting the contribution of the outer medium [i.e., ISM in this paper] to the mass flux in the shell), where v_w is the terminal stellar wind velocity. The streaming velocities in the shell they presented remain still to be obtained numerically. In addition, the physical quantities inferred cannot be applied to the cases of pulsars, W-R stars, blue supergiants, and young O stars for which $v_w > v_*$.

We argue that good approximate analytical solutions to the bow shock can be found coincidentally by considering the centrifugal force term, in spite of the apparent unwieldiness of the equations.

2. APPROXIMATE ANALYTICAL SOLUTIONS

Following most previous works, we assume that the shocked matter is compressed in a thin shell. We discuss two cases, as Dyson (1975) did. In the first case, the shocked ISM and the shocked wind are assumed to mix well. In the second case, they are considered to be separated by a contact discontinuity.

2.1. *The First Case*

Since the shocked materials are mixed in a thin shell, they stream at the same velocity along the surface. Let us adopt

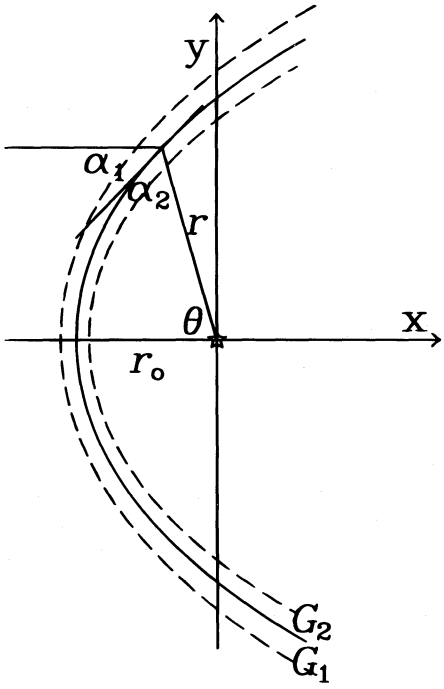

FIG. 1.—Coordinate system set for the bow shock

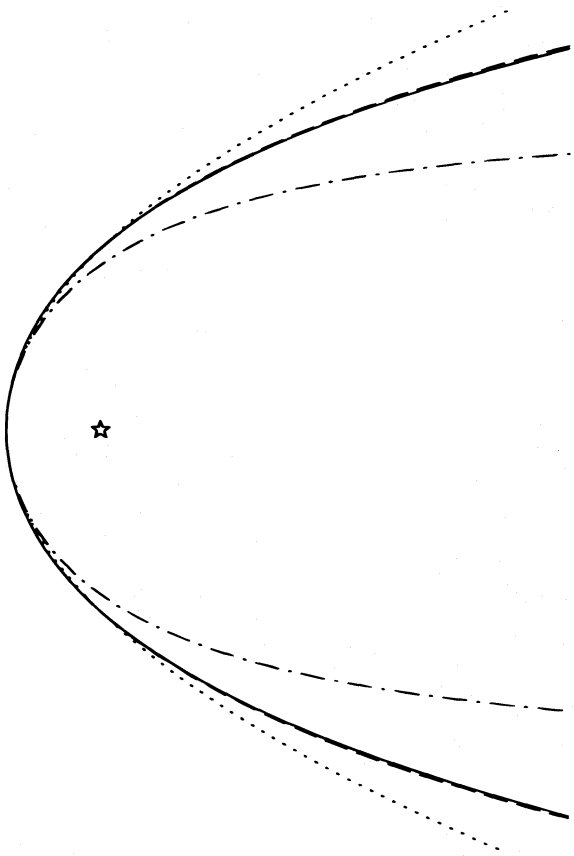

FIG. 2.—Comparison of various analytical solutions of the bow shock morphology with the numerical solution. The open star stands for the star's position. The solid line is the numerical solution. The dashed line is plotted according to equation (10), the dot-dashed line is plotted according to equation (1) (the Dyson 1975 solution), and the dotted line is plotted according to equation (2) (the Mac Low et al. 1991 expansion).

the momentum equations including the centrifugal term, which are used by Chen et al. (1995) with a modification over the divergence term in Huang & Weigert (1982):

$$j_0 \sin^2 \alpha_1 - j_w \sin^2 \alpha_2 = \frac{\sigma v_t^2}{R}, \tag{3}$$

$$j_0 \sin \alpha_1 \cos \alpha_1 + j_w \sin \alpha_2 \cos \alpha_2 = \frac{1}{y}\frac{d}{ds}(\sigma v_t^2 y), \tag{4}$$

where $j_0 \equiv \rho_0 v_*^2$ and $j_w \equiv \dot{M} v_w/(4\pi r^2)$ are the momentum fluxes of the ISM and the stellar wind, respectively, with ρ_0 the mass density of the ISM and $\dot{M}$ the mass-loss rate of the star, s the arc length, σ the surface column mass density of the shell, v_t the tangential velocity of the flow in the shell, α_1 (α_2) the angle of the ISM (wind) momentum vector to the tangent plane, and $R = -(1 + y'^2)^{3/2}/y''$ the curvature radius, with y' and y'' the first and second derivatives of y with respect to x, respectively. The mass continuity equation is

$$\sigma v_t = \frac{j_0}{2v_*} y + \frac{\dot{M}}{4\pi r y}(r + x). \tag{5}$$

The dimensionless form of the above equations in a Cartesian coordinate system is

$$\frac{d\xi}{d\eta} = \frac{1}{\zeta}, \tag{6}$$

$$\frac{d\zeta}{d\eta} = -\frac{\zeta}{\Phi}(1 + \zeta^2)^{1/2}\left[1 - \left(\frac{\eta/\zeta - \xi}{\xi^2 + \eta^2}\right)^2\right], \tag{7}$$

$$\frac{d\Phi}{d\eta} = -\frac{\Phi}{\eta} + \frac{1}{(1 + \zeta^2)^{1/2}}\left[1 + \frac{(\xi + \eta\zeta)(\eta/\zeta - \xi)}{(\xi^2 + \eta^2)^2}\right], \tag{8}$$

$$u = \frac{\eta\Phi}{\eta^2/2 + (v_*/v_w)[1 + \xi/(\xi^2 + \eta^2)^{1/2}]}, \tag{9}$$

where $\xi = x/r_0$, $\eta = y/r_0$, $\zeta = d\eta/d\xi$, $u = v_t/v_*$, and $\Phi = \sigma v_t^2/j_0 r_0$. Here the independent variable has been switched from ξ to η.

We expand the variables ξ, ζ, Φ, and u into Taylor series to the fourth order near the stagnation point ($\eta = y/r_0 \ll 1$):

$$\xi + 1 = \frac{3}{10}\eta^2 + \frac{3}{280}\eta^4, \tag{10}$$

$$\zeta = \left(\frac{3}{5}\eta + \frac{3}{70}\eta^3\right)^{-1}, \tag{11}$$

$$\Phi = \frac{1}{3}\eta^2 - \frac{1}{25}\eta^4, \tag{12}$$

$$u = \frac{2}{3(1 + v_*/v_w)}\eta + \frac{(v_*/v_w - 4)}{50(1 + v_*/v_w)^2}\eta^3. \tag{13}$$

These series are consistent with Bandiera's (1993) equation (16) with $j \to \infty$ there. By the way, the first term on the right-hand side of equation (10) is consistent with the corresponding result in Baranov et al. (1971), i.e., $d^2r/d\theta^2|_{\theta=0} = \frac{2}{5}$, but Aldcroft et al. (1992) improperly found $d^2r/d\theta^2|_{\theta=0} = \frac{1}{2}$ and used it as a boundary condition.

As usual, it would be difficult to find analytical solutions for ordinary differential equations (6)–(8). The key point of this paper is that equation (10) is found not only to apply for $\eta \ll 1$, but also to fit the numerical integration result

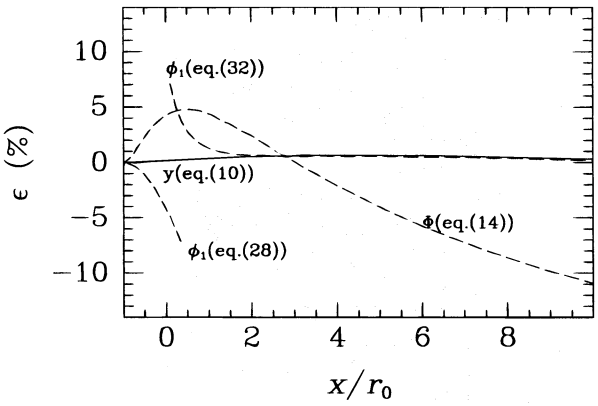

FIG. 3.—Values of ϵ for the analytical solutions. The relative error is defined as $|\epsilon|$.

very well for $\eta > 1$ (see Figs. 2 and 3). In Figure 2, the curve of equation (10) (*dashed line*) is almost pasted on the numerical curve (*solid line*). The relative error (defined as the absolute value of ϵ = [analytical value − numerical value]/[numerical value]) even at $\xi = 100$ does not exceed 7%. Therefore, equation (10) and hence equation (11) are an excellent approximation for the morphology of the bow shock. By comparison, it can be seen in Figure 2 that equation (10) is much better than equation (1), the Dyson solution (*dot-dashed line*). The Taylor expansion (2) (*dotted line*) is not as exact as equation (10) for $\xi < 0$ near the apex.

The other quantity Φ does not hit upon such a coincidence. Figure 4 shows that both the Taylor expansions for Φ to the fourth and the sixth orders diverge quickly after $\xi \gtrsim 0$. However, it can be solved out from equation (7) that

$$\Phi = \frac{(1+\zeta^2)^{1/2}}{\zeta[3/5 + (9/70)\eta^2]}\left[1 - \left(\frac{\eta/\zeta - \xi}{\xi^2+\eta^2}\right)^2\right]. \quad (14)$$

From Figures 3 and 4, one can see that equation (14) fits the numerical values well. Its accuracy is better than 95% for $\xi < 5$ and better than 90% for $\xi < 9$.

With equations (10) and (14), the streaming velocity v_t is known from equation (9). Dividing equation (14) by u^2 then produces the column density σ. The velocity derivation in this way avoids the numerical calculations met by Dyson (1975) and Houpis & Mendis (1980). For $v_w \ll v_*$, this

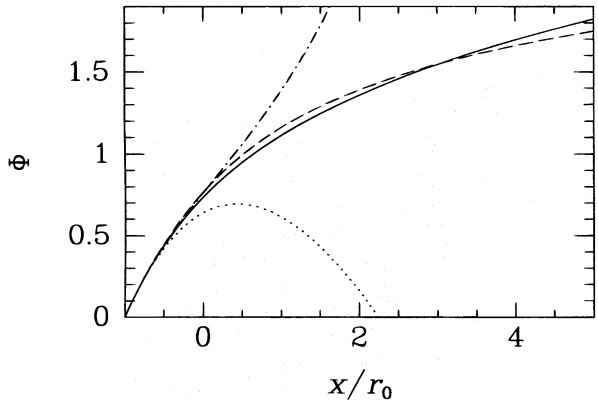

FIG. 4.—Φ as a function of $\xi = x/r_0$. The solid line is the numerical solution of Φ. The dotted line corresponds to equation (12), the dot-dashed line corresponds to the expansion up to the sixth order $\Phi = (1/3)\eta^2 - (1/25)\eta^4 + (39/8750)\eta^6$, and the dashed line corresponds to eq. (14).

velocity,

$$\frac{v_t}{v_w} \approx \frac{\eta\Phi}{1 + \xi/(\xi^2+\eta^2)^{1/2}}, \quad (15)$$

is independent of v_*, consistent qualitatively with those given by Dyson (1975), Houpis & Mendis (1980), and Borkowski et al. (1992). Conversely, the velocity is independent of v_w for $v_w \gg v_*$:

$$\frac{v_t}{v_*} \approx \frac{2\Phi}{\eta} = \frac{2(1+\zeta^2)^{1/2}}{\zeta[(3/5)\eta + (9/70)\eta^3]}\left[1 - \left(\frac{\eta/\zeta - \xi}{\xi^2+\eta^2}\right)^2\right]. \quad (16)$$

2.2. *The Second Case*

In the second case, the surface we discuss is the contact discontinuity separating the two shocked matter layers G_1 and G_2, between which there is assumed to be no matter exchange. Assume that the flows in shells G_1 and G_2, with the column densities σ_1 and σ_2, stream at uniform velocities v_1 and v_2, respectively. The momentum equations for the two layers are

$$j_0 \sin^2\alpha_1 - j_w \sin^2\alpha_2 = \frac{\sigma_1 v_1^2 + \sigma_2 v_2^2}{R}, \quad (17)$$

$$j_0 \sin\alpha_1 \cos\alpha_1 = \frac{1}{y}\frac{d}{ds}(\sigma_1 v_1^2 y), \quad (18)$$

$$j_w \sin\alpha_2 \cos\alpha_2 = \frac{1}{y}\frac{d}{ds}(\sigma_2 v_2^2 y). \quad (19)$$

The mass equations are

$$\sigma_1 v_1 = \frac{j_0}{2v_*} y, \quad (20)$$

$$\sigma_2 v_2 = \frac{\dot{M}}{4\pi r y}(r + x). \quad (21)$$

We express these equations in dimensionless form as

$$\frac{d\zeta}{d\eta} = -\frac{\zeta(1+\zeta)^{1/2}}{\phi_1 + \phi_2}\left[1 - \left(\frac{\eta/\zeta - \xi}{\xi^2+\eta^2}\right)^2\right], \quad (22)$$

$$\frac{d\phi_1}{d\eta} = -\frac{\phi_1}{\eta} + \frac{1}{(1+\zeta^2)^{1/2}}, \quad (23)$$

$$\frac{d\phi_2}{d\eta} = -\frac{\phi_2}{\eta} + \frac{(\xi+\eta\zeta)(\eta/\zeta - \xi)}{(1+\zeta^2)^{1/2}(\xi^2+\eta^2)^2}, \quad (24)$$

$$u_1 = \frac{2\phi_1}{\eta}, \quad (25)$$

$$u_2 = \frac{\eta\phi_2}{1 + \xi/(\xi^2+\eta^2)^{1/2}}, \quad (26)$$

where $\phi_1 = \sigma_1 v_1^2/j_0 r_0$, $\phi_2 = \sigma_2 v_2^2/j_0 r_0$, $u_1 = v_1/v_*$, and $u_2 = v_2/v_w$. The similarities in the form of equation (25) and (26) to equations (16) and (15) are worth noting. It can be found that equation (22) and the sum of equations (23) and (24) are the same as equations (7) and (8) in the first case, with

$$\Phi = \phi_1 + \phi_2. \quad (27)$$

Therefore, equations (10) and (11) are still the solutions that determine the morphology of the contact discontinuity. In fact equations (3) and (4), which give the bow shock shape and momentum flux, are closed on these quantities, and

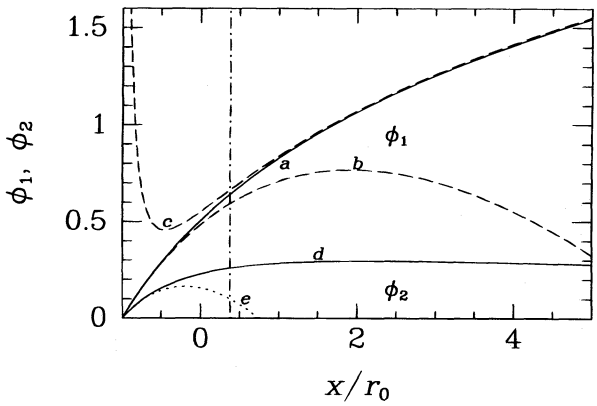

FIG. 5.—Plot of ϕ_1 and ϕ_2 as functions of $\xi = x/r_0$. The top three lines are for ϕ_1, and the bottom two lines are for ϕ_2. The solid line a is the numerical solution of ϕ_1. The dashed line b corresponds to eq. (28), and the dashed line c corresponds to eq. (32). The solid line d is the numerical solution of ϕ_2, and the dotted line e corresponds to eq. (29). The vertical dot-dashed line marks the location for $\eta = 2$.

they do not require any further assumption on how the velocity profile is across the bow shock. Let us make the following Taylor polynomial expansion for $\eta \ll 1$:

$$\phi_1 = \frac{1}{5}\eta^2 - \frac{57}{4375}\eta^4 , \tag{28}$$

$$\phi_2 = \frac{2}{15}\eta^2 - \frac{118}{4375}\eta^4 , \tag{29}$$

$$u_1 = \frac{2}{5}\eta - \frac{114}{4375}\eta^3 , \tag{30}$$

$$u_2 = \frac{4}{15}\eta - \frac{61}{4375}\eta^3 . \tag{31}$$

Figures 3 and 5 show that equation (28) fits the numerical values well for $\eta < 2$ or $\xi < 0.37$. Both equations (28) and (29) diverge quickly for larger η. For $\eta \gtrsim 2$, however, we an obtain an asymptotic solution of ϕ_1 by integrating equation (23):

$$\phi_1 = \frac{1}{2}\eta - \frac{1225}{126\eta}\left[\frac{1}{\eta^2 + 14} - \frac{1}{14}\ln\left(1 + \frac{14}{\eta^2}\right)\right] - \frac{1.18}{\eta} , \tag{32}$$

where the number 1.18 is determined from the numerical values. In the derivation, the approximation $(1 + \zeta^2)^{-1/2} \approx 1 - \zeta^2/2$ and equation (11) have been used. In Figures 3 and 5, one sees that, for $\eta \gtrsim 2$, equation (32) fits the numerical result very well. The combination of equations (28) (for $\eta < 2$) and (32) (for $\eta \gtrsim 2$) has an accuracy $\gtrsim 94\%$. In addition, ϕ_2 for large η can be obtained via the relation (27).

3. CONCLUSION

The general quantities describing the thin-shell bow shock are worked out analytically with higher accuracy than previous analytical solutions by taking into account the centrifugal force term. The two ideal cases are considered: the shocked wind and the shocked ISM are mixed and separated, respectively. The morphology of the bow shock can be determined by equation (10). The quantity σv_t^2 for the first case is given by equation (14). The quantity $\sigma_1 v_1^2$ for the second case is given by equations (28) and (32). The density in the shell and hence the thickness of the shell are influenced sensitively by concrete thermal condition, external ionization, MHD effects, instabilities, and even chemical reaction, and they should be modeled separately.

Note added in manuscript.—We read a preprint of Wilkin (1996) after the submission of this paper. In his Letter, Wilkin uses an elegant approach to find the exact analytical solutions for a one-layer bow shock. Our approximate solutions in the one-layer case (§ 2.1) are in agreement with his solutions: equation (10) in this paper can also be obtained by expanding his equation (9). Still, equation (10) seems to be an effective, simple expression for the bow shock's shape in a Cartesian system. Note that we have also presented physical quantities for the two-layer case (§ 2.2), which is not discussed by Wilkin.

Y. C. wishes to thank Q. Zhang for interesting discussions. R. B. wishes to thank F. P. Wilkin for having acquainted him with his preprint. This work was carried out on a Sun 4/280 computer at the Data Analysis Center of the Department of Astronomy, Nanjing University. This work is supported by a grant from the National Natural Science Foundation of China and a grant from the Climbing Project of the State Scientific Commission of China.

REFERENCES

Aldcroft, T. L., Romani, R. W., & Cordes, J. M. 1992, ApJ, 400, 638
Bandiera, R. 1993, A&A, 276, 648
Baranov, V. B., Krasnobaev, K. V., & Kulikovksii, A. G. 1971, Soviet Phys. Dokl., 15, 791
Baranov, V. B., Lebedev, M. G., & Ruderman, M. S. 1979, Ap&SS, 66, 441
Borkowski, K. J., Blondin, J. M., & Sarazin, C. L. 1992, ApJ, 400, 222
Chen, Y., Wang, Z.-R., & Qu, Q.-Y. 1995, ApJ, 438, 950
Dyson, J. E. 1975, Ap&SS, 35, 299
Houpis, H. L. F., & Mendis, D. J. 1980, ApJ, 239, 1107
Huang, R. Q., & Weigert, A. 1982, A&A, 116, 348
Mac Low, M.-M, Van Buren, D., Wood, D. O. S., & Churchwell, E. 1991, ApJ, 369, 395
Matsuda, T., Fujimoto, Y., Shima, E., Sawada, K., & Inaguchi, T. 1989, Prog. Theor. Phys., 81, 810
Raga, A. C., & Cabrit, S. 1993, A&A, 278, 267
Raga, A. C., Cabrit, S., & Cantó, J. 1995, MNRAS, 273, 422
Van Buren, D., Mac Low, M.-M., Wood, D. O. S., & Churchwell, E. 1990, ApJ, 353, 570
Van Buren, D., & McCray, R. 1988, ApJ, 329, L93
Wang, L., Dyson, J. E., & Kahn, F. D. 1993, MNRAS, 261, 391
Wilkin, F. P. 1996, ApJ, 459, L31